Microfluid Nanofluid (2010) 9:593–611
DOI 10.1007/s10404-010-0607-2

REVIEW

Induced-charge electrokinetic phenomena

Yasaman Daghighi · Dongqing Li

Received: 15 January 2010 / Accepted: 18 March 2010 / Published online: 7 April 2010

Abstract The induced-charge electrokinetic (ICEK) phenomena are relatively new area of research in microfluidics and nanofluidics. Different from the traditional electrokinetic phenomena which are based on the interactions between applied electric field and the electrostatic charge, the ICEK phenomena result from the interaction of the applied electric field and the induced charge on polarisable surfaces. Because of the different underline physics, ICEK phenomena have many unique characteristics that may lead to new applications in microfluidics and nanofluidics. In this paper, we review the major advancement of research in the field of ICEK phenomena, discuss the applications and the limitations, and suggest some future research directions.

Keywords Induced-charge electrokinetic phenomena · Polarisable surfaces/particles · Conductive surfaces/particles · Heterogeneous (Janus) particles · Electro-osmotic · Electrophoresis

1 Introduction

Electrokinetic phenomena provide many popular non-mechanical techniques in microfluidics and lab-on-a-chip devices (Stone et al. 2004), such as pumping, mixing and particle separation. Generally, electrokinetic phenomena (electrically driven liquid flow and particle motion) are produced by the interactions of the applied electric field with the surface charge or its ionic screening clouds (Saville 1977; Anderson 1989). Typical electrokinetic phenomena include: (i) electro-osmosis, liquid flow generated by an applied electric field force acting on the ionic charge cloud near a solid surface; (ii) electrophoresis, the motion of a charged particle in a liquid under an applied electric field.

The 'classical' electrokinetics (EK) was first developed in colloid sciences and surface chemistry (Hunter 2001; Lyklema 1995; Anderson 1989) and has entered the microfluidics area over the past 10–15 years (Li 2004; Li 2008). Most studies of EK have assumed linear response to the applied electric field, and fixed static surface charge (Li 2004; Li 2008; Schoch et al. 2008; Saville 1977). There are a number of shortcomings for linear electrokinetic phenomena. For example, electrophoresis cannot separate particles by size or shape for particles with fixed, uniform zeta potential in free solution; and strong electric field must be applied to the whole system to achieve the necessary field strengths, generating Joule heating and having little direct control over local fields and flows within microchannels (Bazant and Squires 2010).

Recently, studies of induced-charge electrokinetics (ICEK) phenomena have drawn more and more interest. In the ICEK phenomena, the solid surface does not necessarily to have electrostatic charge, but must be able to be induced to have charge. The interaction of the applied electric field with the induced charge can generate various phenomena that are not available in the cases of electrostatic surface charge. Electrokinetic flows around polarizable particles have been studied since the pioneering work of Levich (1962). The behaviour of polarizable colloids in an electric field was previously studied in a series of papers by Dukhin and coworkers (Simonov and Dukhin 1973; Gamayunov et al. 1986; Dukhin and Murtsovkin 1986; Dukhin 1986), the

Y. Daghighi · D. Li (✉)
Department of Mechanical and Mechatronics Engineering, University of Waterloo, Waterloo, ON N2L 3G1, Canada
e-mail: dongqing@mme.uwaterloo.ca

results were later summarized by Murtsovkin (1996). Experimental observations of this induced charge flow were reported by Gamayunov et al. (1992). They were the first group who predicted the quadrupolar-induced charge electro-osmotic flow around an ideally polarizable sphere in a uniform electric field, and the resulting relative motion of two spheres. Later on, Ramos et al. (1999) discovered alternating-current electro-osmotic flow (AC-EOF) over microelectrodes. This idea was proposed to be used as low-voltage microfluidic pumping by Ajdari (2000) one year later. The experimental results produced by Green et al. (2000, 2002), Gonzalez et al.(2000), Brown et al. (2001), Studer et al. (2004) and others with focus on non-linear AC electrokinetics in microfluidics (Bazant 2008; Bazant et al. 2009) and confirmed the findings of the Ramos et al. (1999) and Ajdari (2000). In 2004, Bazant and Squires (2004) and Squires and Bazant (2004) used the term 'induced-charge' flows for the first time to describe the physical mechanism of applied electric field acting on its induced charge near a polarizable surface. They also noted that the effect described earlier in the Russian literature on metallic colloids by Murtsovkin (1996) and Gamayunov et al. (1992) is essentially the same.

Induced-charge electro-osmotic flow (ICEOF) is generated when an external electric field polarizes a polarizable solid object placed in an electrolytic solution (Gamayunov et al. 1992; Ramos et al. 1999; Ajdari 2000; Green et al. 2000; Gonzalez et al. 2000; Green et al. 2002; Brown et al. 2001; Studer et al. 2004; Bazant 2008; Bazant et al. 2009; Squires and Bazant 2004; Bazant and Squires 2004; Levitan et al. 2005). Initially, the object acquires a position-dependent potential difference relative to the bulk electrolyte. However, this potential is screened out by the counter-ions in the electrolyte by the formation of an electric double layer (EDL) at the surface of the object. The ions in the diffusive part of the double layer then electro-migrate under the external electric field tangential to the surface of the object, and drag the liquid molecules to move by the viscous effect. The electro-osmotic flow (EOF) is thus established. The ICEOF effect may be utilized in microfluidic devices for fluid manipulation, as proposed in 2004 by Bazant and Squires (2004). Theoretically, various simple shapes have been analysed for their ability to pump and mix liquids (Bazant and Squires 2004). Experimentally ICEOF was observed and the basic model was validated using particle image velocimetry in 2005 (Levitan et al. 2005) and later it was used for microfluidic mixing, and a number of triangular objects were used as passive mixers (Harnett et al. 2008). Recent research includes using ICEOF for mixing and flow regulating (Wu and Li 2008a, b) and promoting stirring and chaotic advection (Zhao and Bau 2007a, b), particle–wall interaction (Zhao and Bau 2007b; Yariv 2009; Wu and Li 2009) and particle–particle interaction (Saintillan 2008; Wu et al. 2009), non-spherical particles (Yariv 2005a, b; Squires and Bazant 2006; Saintillan et al. 2006a; Yossifon et al. 2007; Yariv 2008) and suspension dynamics (Saintillan et al. 2006a, b; Rose et al. 2007). General mobility relations of induced-charge electrophoresis (ICEP) for homogenous non-spherical conductive particles have been derived (Yariv 2005a, b) and two-dimensional ICEP motion has been calculated for arbitrary shape perturbations (Squires and Bazant 2006), as well as rod-like spheroidal shapes (Saintillan et al. 2006a, b).

ICEK phenomena occur over all polarizable surfaces. In fact, the case of a perfectly conductive surface represents the limit of ideally polarizable materials. Accordingly, the induced-charge phenomenon is also pertinent for a variety of dielectric materials (Thamida and Chang 2002; Yossifon et al. 2006), as well as biological cells (Dukhin and Murtsovkin 1986). ICEK phenomena have a variety of advantages some are unique to ICEK, for example,

(1) *Zeta potential control*: In ICEK, the induced zeta potential ζ_i of the EDL strongly depends on the applied electrical field, one can in principle 'tune' and predict ζ_i through appropriate field strength. This control enables the predictive and rational design of ICEK devices and process control.
(2) *Non-linear dependence on the applied electric field*: Because of the dependence of the induced zeta potential ζ_i on the applied electrical field, E, the resulting velocity of electro-osmotic flow and electrophoretic motion is proportional to E^n, where $n > 1$. In comparison with the traditional EOF, this implies that the velocity of ICEOF is much higher.

In this article, we review recent advances in ICEK, focusing on key papers from the past several years. We begin with a sort summary of the classical electrokinetic phenomena, the related assumptions and limitations. Then, we introduce the basics theory of the ICEK phenomena, and some key formulations. The key findings of both ICEO and ICEP are reviewed. Throughout this review article, we emphasize the applications and the limitations of the current research in this field. Finally, we provide suggestions for future experimental and theoretical research in ICEK phenomena.

2 Electrokinetic phenomena

2.1 Classical electrokinetic phenomena

The classical EK involves the interactions between an externally applied electric field and the EDL near a non-conductive object with electrostatic charge. When a solid

surface is in contact with an electrolyte solution, the static charge on the solid surface will attract the counter-ions and repel the co-ions in the liquid. The charges on the solid surface and the re-arranged ions in the liquid form the EDL. Immediately next to the charged solid surface, there is a layer of counter-ions that are strongly attracted to the solid surface and are immobile. This layer is called the compact layer. From the compact layer to the electrically neutral bulk liquid, the net charge (the excess counter-ions) density gradually reduces to zero. Ions in this region are affected less strongly by the electrostatic interaction and are mobile. This region is called the diffuse layer of the EDL. The electric potential at the boundary between the compact layer and the diffuse layer (i.e., the shear plane) is called the zeta potential, ζ, the potential drop across the diffuse layer of the EDL. An externally applied electric field gives a body force on the net charge in the diffuse layer of the EDL. EK phenomena are categorized into two main groups: (i) electro-osmosis, the motion of liquid relative to the charged solid surface; (ii) electrophoresis, the motion of the charged particle relative to the liquid.

When an external electric field is applied along a microchannel filled with an aqueous solution, the applied electric field exerts a body force on the excess counter-ions in the EDL, driving the ions and thus the bulk liquid into motion. The resulting liquid flow is called the electro-osmotic flow (EOF). If the EDL thickness is small in comparison with the microchannel dimensions, the flow appears to slip at the solid–liquid interface and causes a plug-like flow profile in a microchannel. The local slip velocity is given by the well-known Helmholtz–Smoluchowski equation (Hunter 1981)

$$\vec{u}_{\mathrm{eo}} = -\frac{\varepsilon\zeta}{\mu}\vec{E} \tag{1}$$

where ε is the dielectric permittivity, ζ is the zeta potential, μ is the viscosity of the liquid and $\mu_{\mathrm{eo}} = -\frac{\varepsilon\zeta}{\mu}$ is the so-called electro-osmotic mobility of the liquid.

When a charged particle is freely suspended in a bulk electrolyte solution, the velocity of steady-state electrophoretic motion of the particle can be obtained by balancing the electric body force and the flow friction force on the particle. In the thin double-layer limit, the electrophoretic velocity of particle is given by Helmholtz–Smoluchowski formula (Hunter 1981)

$$\vec{u}_{\mathrm{ep}} = \frac{\varepsilon\zeta}{\mu} \quad \vec{E} = \mu_{\mathrm{ep}}\vec{E} \tag{2}$$

where $\mu_{\mathrm{ep}} = -\frac{\varepsilon\zeta}{\mu}$ refers to the electrophoretic mobility of particle.

In general, the classical electrokinetic phenomena involve a non-conductive surface with fixed electric charge, or equivalently, fixed zeta potential. Therefore, as indicated by Eqs. 1 and 2, the velocity of the electrokinetic motion is linearly proportional to the applied electric field E. This is the reason that these electrokinetic phenomenon are sometimes referred to as 'linear EK', i.e. $\vec{u} \propto \vec{E}$.

The classical theory of EK, dating back over a century to Smoluchowski, employs many assumptions to model an electrokinetic phenomenon such as homogeneous dilute electrolytes which is unbounded, non-polarizable, uniformly charged, rigid spherical particles which is much larger than the thickness of the EDL, very far from any walls or other particles, and uniform and weak field. However, in practice there are many cases where these assumptions may cause significant deviation from the true physics. For instance, most materials are polarizable to some degree. Thus, the surface charge is generally not fixed. This leads to a broad class of non-linear electrokinetic phenomena, where the electric field induces surface charge and interacts with the EDL of the induced charge to produce non-linear electrophoretic motion, $\vec{u} = \vec{f}(\vec{E})$.

2.2 ICEK phenomena

The basic difference between the traditional EK and the ICEK is the origin of the surface charge. In classical EK, the surface charge is static and most time fixed. However, the situation will be very different if the solid surface is polarizable and electrically conductive. In ICEK, the surface charge is induced by the applied electric field, although the surface may have static charge in addition. To understand the basic principles of ICEK, let us consider a simple case as shown in Fig. 1: an arbitrary-shaped object that is ideally polarizable and conductive is immersed in an aqueous solution and under a uniform electric field, $\vec{E}_0$.

Once the electric field is suddenly applied over the object, a non-zero current $J = \sigma\vec{E}$ goes from the aqueous solution to the conductive surface of the conductivity σ. Thus, the electric field lines initially intersect the conductive surface at right-angles (Fig. 1a). The current drives positive charges into a thin layer on one side of the conductor and the negative charges into the other, inducing an equal and opposite surface charge q on the conductive surface and also attracting equal and opposite image charges within the conductor itself. These surface charges in turn attract the counter-ions in the liquid. Consequently, a dipolar screening cloud adjacent to the solid–liquid surface is forming. The induced surface charge q and the corresponding induced zeta potential ζ_i change with time (Bazant and Squires 2004; Squires and Bazant 2004), and are given by

$$\frac{\mathrm{d}q}{\mathrm{d}t} = \vec{J}\cdot\vec{r} = \sigma\,\vec{E}\cdot\vec{r} \tag{2}$$

and

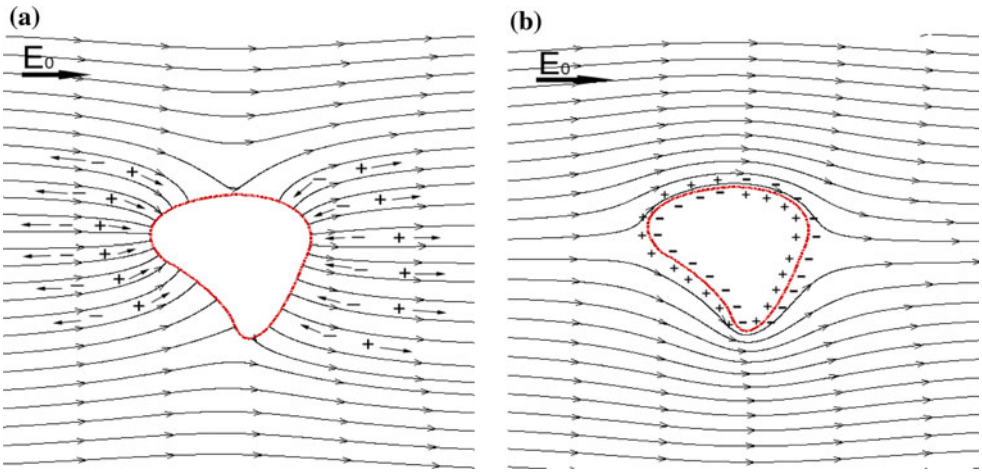

Fig. 1 Schematic of the charging process of a conductive object in a uniform applied electric field: **a** initial electric field, **b** steady-state electric field and the induced dipolar EDL (*source*: Wu and Li 2009b)

$$\frac{\mathrm{d}\varsigma_i}{\mathrm{d}t} = \frac{\lambda_\mathrm{D}\,\sigma}{\varepsilon}\vec{E}\cdot\vec{r} \tag{3}$$

where λ_D is the Debye length (Hunter 1981) and ζ_i and ε are the induced zeta potential and the dielectric permittivity of the solution, respectively.

Because of the presence of the screening charge cloud, the electric field lines are expelled and the ionic flux into the charge could is reduced. Eventually, when the conductor is fully polarized and reaches a steady-state, the conductor behaves like an insulator because an induced dipolar double layer is formed, as shown in Fig. 1b. Then, a steady-state electric field is established. This steady-state electrostatic configuration is equivalent to the no-flux electrostatic boundary condition assumed in standard electrokinetic analysis. The external applied electric potential ϕ_e at this steady-state is governed by Laplace's equation

$$\nabla^2\phi_\mathrm{e} = 0 \tag{4}$$

The charging time for setting up this steady field is quite small (on the order of 10^{-4} s) for a highly polarizable conductor (Bazant and Squires 2004; Squires and Bazant 2004) and is negligible in comparison with the characteristic time of most microfluidic transport processes.

Evaluating the zeta potential of the induced charge is critical to calculate the velocity of the ICEK motion. For relatively simple and regular geometries, there exist analytical expressions of the induced zeta potential. For instance, Squires and Banzant have derived an exact analytical formulation of the induced zeta potential on the surface of a 2D circular cylinder (Bazant and Squires 2004) given by

$$\zeta_i(\theta) = 2E_0 a\cos\theta \tag{5}$$

where θ is angular coordinate and a is the radius of the cylinder. However, for a surface of a complex or irregular shape, there is no simple analytical solution for the distribution of the induced zeta potential. Thus, a numerical scheme is needed to relate the induced zeta potential with the external applied field. Considering an ideally polarizable conductor, the steady-state induced zeta potential distribution ζ_i can be numerically determined by the following consideration (Wu and Li 2008a).

The induced screening cloud generates a local electric field and acts as an insulating shell over the conductive surface so that the field lines of the externally applied electric field cannot intersect the surface. Thus, the local strength of the induced field E_i on the conductive surface, i.e. the local potential gradient along the surface, should be of the same magnitude as that of the externally applied electrical field E_e, i.e.

$$|E_i| = |E_e| \tag{6}$$

Because the image charges in the conductor have an opposite sign to that of the ions attracted at the conductive surface from the liquid, the induced electric field at the conductor–liquid interface should be in the opposite direction to that of the external field, i.e.

$$E_i = -E_e \tag{7}$$

or

$$\nabla\zeta_i = -\nabla\phi_\mathrm{e} \tag{8}$$

where ϕ_e is the local externally applied electric potential given by Eq. 4.

Assuming that the conductor is initially uncharged, the integration of the induced charge over the whole conductive surface should be zero because of the initial electric neutrality of the surface. Thus, the integration of the induced zeta potential over the conductive surface should be zero, i.e.

$$\oint_S \zeta_i \mathrm{d}s = 0 \tag{9}$$

where S is the conductive surface in the applied electric field. If the conductive surface is initially charged, the final steady-state zeta potential distribution is simply a superposition of the initial equilibrium zeta potential $\zeta_0 = \zeta(t = 0)$ and the induced zeta potential ζ_i.

If we limit our attention to the case of thin double layer and small Dukhin number (i.e., surface conduction is negligible compared to the bulk conduction), and no electrochemical reactions are present at the conductor–liquid interface, the above conditions are valid. The following method can be used to numerically calculate the induced zeta potential distribution on the conductive surfaces from the known external electric potential ϕ_e. Directly integrating Eq. 8, the local induced zeta potential is obtained as:

$$\zeta_i = -\phi_e + \phi_c \tag{10}$$

where ϕ_c is a constant correction potential. By inserting Eq. 10 into Eq. 9, we can evaluate the correction potential as:

$$\phi_c = \frac{\int_S \phi_e dA}{A} \tag{11}$$

where A is the area of the entire surface of the conductive object. Equations 10 and 11 provide a simple numerical method to calculate the final steady-state induced zeta potential distribution on the conductive surfaces with arbitrary geometries.

3 ICEOF

ICEOF is generated when an external electric field polarizes an object in an electrolytic solution. A dipolar EDL of thickness λ_D is formed at the surface of the polarisable object. The excess counter-ions in the diffuse part of the double layer electromigrate in the external electric field and drag the liquid to move by viscous forces. Once the electric field is applied, the conductive surface is polarized and reaches the steady-state almost immediately. At the steady-state, the dipolar double layer acts as the screening cloud to the externally applied field and is equivalent to the no-flux electrostatic boundary condition in standard EK. The velocity of the ICEOF is given by the Smoluchowski equation:

$$u_{eo} = \frac{\varepsilon \zeta_i}{\mu} E \tag{12}$$

However, it should be noted that the zeta potential in the above equation is the induced zeta potential $\zeta_i = f(E)$

The research in ICEOF has primarily been conducted in the field of colloids, where experimental and theoretical studies have been carried out on the EDL and induced dipole moments around spheres in electric fields, as reviewed by Dukhin (1986) and Murtsovkin (1996). In recent years, in the studies of microfluidic systems, electrokinetically driven liquid motion has been used for pumping, mixing, concentration gradient generation, separation and sorting. From a microfabrication point of view, planar electrodes are easy to fabricate and integrate in microfluidic systems. For this reason much research has been focused on the motion of liquids above planar electrodes. Building on the work of Soni et al. (2007), Pascall et al. (2010) developed a novel automated system, capable of measuring and characterizing ICEO flows over various surfaces with various electrolytes, under approximately 1,000 conditions per day. In particular, they used microparticle image velocimetry to measure the ICEO slip velocity just above a 50-μm wide gold electrode, deposited onto the floor of a microchannel (Fig. 2). To specifically test the effects of surface contamination on ICEO flows, Pascall et al. 'controllably contaminated' the electrode with a SiO_2 film of various known thicknesses, and directly compared the predicted ICEO flows against measured values. Accounting for the physical dielectric effect of the contaminant, as well as the 'buffer capacitance' of ion adsorption onto reactive sites on the surface (Squires and Bazant (2006)), they obtained quantitative agreement between the theory and the experiments. While their study was within the low zeta potential limit, their techniques

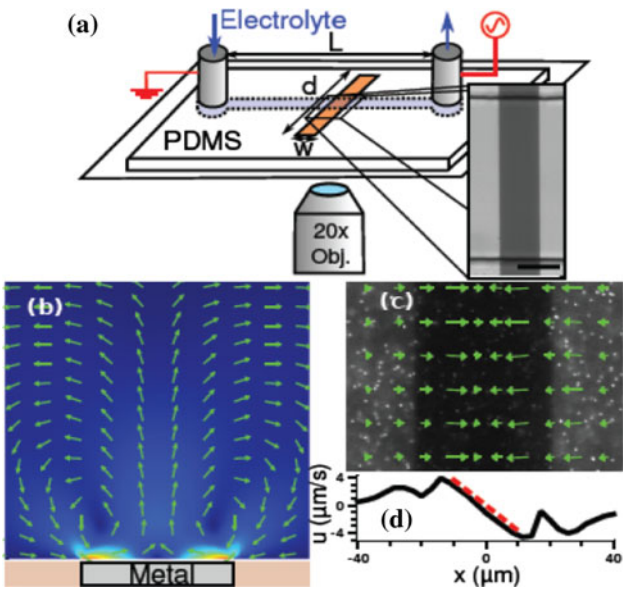

Fig. 2 **a** The experimental system of Pascall and Squires (2010) for systematic comparison of theory and experiments of ICEOF studies. Thin film materials were deposited on metal electrode—a planar gold strip (50 μm) placed perpendicularly to a PDMS microchannel. **b** AC field was applied, driving two counter-rotating vortices. (**c**, **d**) Micro-PIV measurements just above the metal strip and an ICEK slip velocity that varies linearly with distance from the strip centre (*source*: Pascall and Squires 2010)

enable high-throughput measurement and characterization of any material that can be deposited onto a conductive substrate, under a wide range of experimental conditions.

3.1 ICEOF mixing

Generally, flows in microchannels are laminar ($Re \ll 1$) because of the slow velocity and small characteristic length scale. Mixing of different fluids in microchannels is a challenging issue. Various methods have been developed to introduce perturbation into the flow to enhance the flow mixing. ICEOF has unique flow characteristics that can be used for flow mixing enhancement.

Consider an electric conductive object is placed in an electrolyte solution in an external electric filed. As described above, once the induced dipolar double layer is formed around the conducting surface, the externally applied field exerts a body force on the excess counter-ions in the diffuse layer of the EDL in the liquid, driving the ions and the liquid into motion (Fig. 3). The resultant electrokinetic flow appears to slip just outside the EDL of thickness λ_D and the slip flow velocity varies proportionally to the local tangential electric field

$$\vec{u} = -\frac{\varepsilon \varsigma_i}{\mu}\vec{E} \tag{13}$$

where μ is the fluid viscosity. It is important to recognize that the induced EDL is dipolar. That is, the net charge in the EDL facing the electric field is positive, and the net charge of the EDL on the opposite side is negative, as shown in Fig. 3. Under the same applied electric field, the EOFs in these parts of the EDL are in different directions. The non-uniform EOF results in vortices near the solid–liquid interface. As this figure illustrates, the direction of each vortex is opposite to the other one. The vortices generated by the ICEOF can be used to enhance the flow mixing in microfluidics.

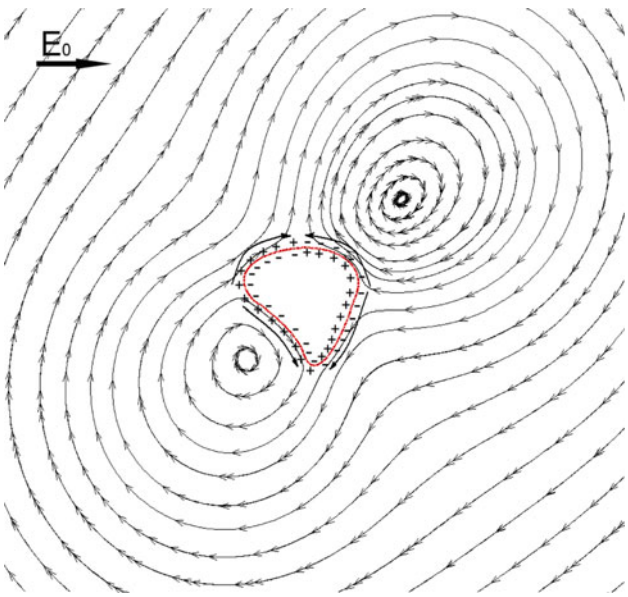

Fig. 3 Generation of vortices around an arbitrary polarizable surface (*source*: Wu and Li 2009a)

Theoretical work has shown that ICEOF-based micromixing can be enhanced by broken symmetries (Zhao and Bau 2007a, b), temporal modulation to achieve chaotic streamlines (Gregersen et al. 2009), topological shape optimization (Yossifon et al. 2006), or by the introduction of polarisable hurdles in dielectric microchannels (Wu and Li 2008a). Bazant and Squires (2004) proposed the use of AC-ICEO flow around metallic microstructures to generate vortices for microfluidic mixing (Squires and Bazant 2004). Wang et al. (2006) demonstrated experimentally a mixing system in a microfluidic reservoir smaller than 10 μl using AC electro-osmosis. Their system includes three circular reservoirs (3 mm in diameter) connected by a 1 mm × 1 mm × 1 mm channel. Two side-reservoirs were used to insert the electrodes to avoid the bubble generation at low-frequency AC field. Those two side-reservoirs are connected to the middle one via microchannels. The middle well is used as the mixing region. Although their designed system is very simple, a high voltage is applied to manipulate the flow. However, their results showed good improvement in mixing with reduced mixing time.

In 2008, two groups reported the first experimental demonstrations of microfluidic mixing by ICEO flow around metallic microstructures. Harnett et al. (2008) integrated an array of gold-coated posts of triangular cross section in a microchannel with electrodes applying a low-frequency AC field on the side walls. The post-array mixer was placed at the junction of two Y-channels, and programmable on/off mixing of two different streams of dilute electrolytes was demonstrated. As shown in Fig. 4, they developed a new microfabrication process for vertical sidewalls having conductive metal coatings and embedded electrodes. The chip has a channel of 50 μm in depth, 10000 μm in length and 1000 μm in width. At the centre of the channel is a 10 by 5 array of posts 150 μm in diameter. A gold coating was applied to the lateral surfaces of the posts for the purposes of the ICEO experiments. Good agreement with theoretical predictions was noted, albeit with a 'correction factor' of 0.25.

Wu and Li (2008a, b) reported simulations and experiments on ICEOF mixing when flows pass electrically conductive hurdles in microchannels. Their simulation demonstrated that the species mixing can be enhanced significantly by the vortices generated near the hurdles. When the conductive hurdles are immersed in the applied electric field, a non-uniform distribution of zeta potential

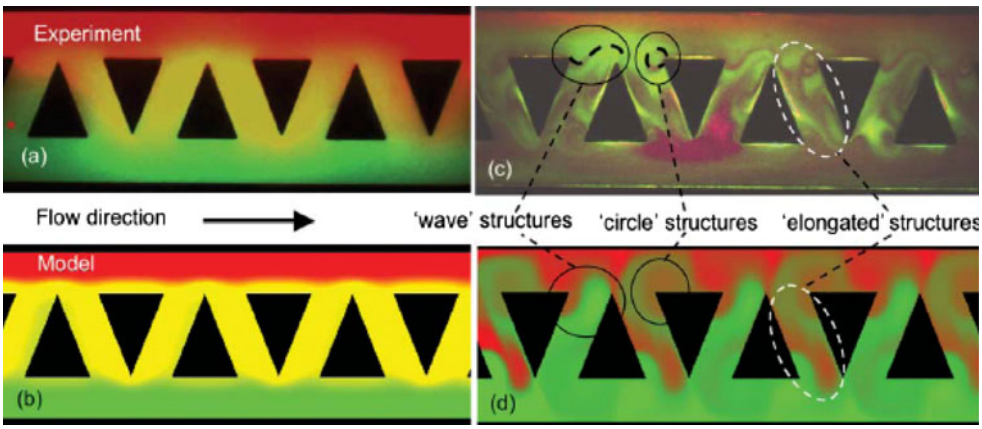

Fig. 4 Experimental (**a**, **c**) and numerical simulation (**b**, **d**) results for the distribution of *red* and *green* fluorescent beads after loading (**a**, **b**) during mixing (**c**, **d**) (*source*: Harnett et al. 2008)

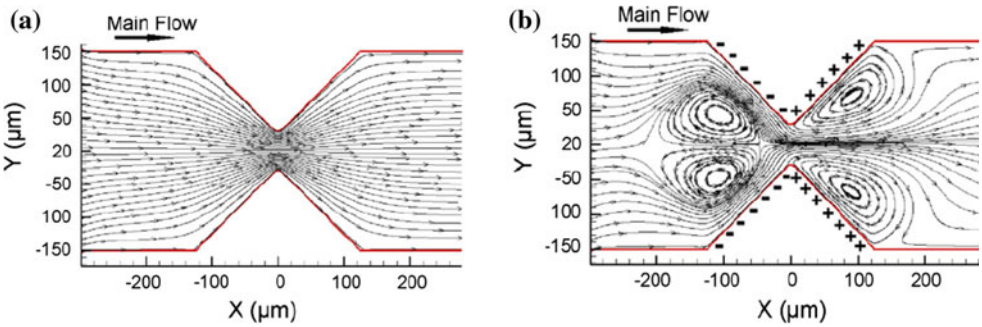

Fig. 5 Electro-osmotic flow field in a microchannel near **a** a pair of non-conductive triangular hurdles and **b** a pair of conductive triangular hurdles (*source*: Wu and Li 2008a)

will be induced on the conductive surfaces, causing a varying driving force of the EOF. Consequently, the EOF velocity on the conductive surfaces changes with position, resulting in a non-uniform flow field. Figure 5 shows the flow fields for the case of conductive hurdles and the case of non-conductive hurdles, respectively. As one can see, the most notable feature in the flow field, as Wu and Li (2008b) illustrated, is that the vortices generated near the conductive hurdles. Due to the oppositely charged surfaces, flow circulations are generated near the embedded hurdles in the channel. The opposite signs of the induced zeta potential indicate opposite EOF driving forces, which are responsible for the flow circulations (Wu and Li 2008a). Their results illustrated that (1) the degree of enhancement highly depends on the hurdle geometry; (2) the rectangle hurdle produces the strongest mixing effect; (3) the mixing can be further enhanced by adding more conductive hurdles in series in the microchannel to generate more vortices.

They fabricated the microchannel chips by soft lithography technique using two polydimethylsiloxane (PDMS) slabs, the top layer has the microchannel structure, and the bottom layer forms the substrate. The hurdles (GeSim Ltd, Dresden, Germany) used in their study are made of silicon and all have a triangular-shaped head of 200 μm in bottom-width, 125 μm in height and 36 μm in thickness. The non-conducting silicon hurdles are coated with 1.5 μm SiO_2 insulation layer and have a thin-platinum-film (150 nm) covered triangle head. The conducting hurdle head were inserted into the microchannel through the pre-designed insertion space in the channel. As shown in Fig. 6, the microchannel had two branches at the left, connected with the anode of a DC power supply, for parallel delivery of two different solutions. The right single branch forms a mixing channel and is connected with the cathode of the DC power source. One of the inlet streams is a sodium carbonate/bicarbonate buffer, and the other inlet stream is a fluorescent dye (Fluorescein) solution for visualizing the mixing effects. Figure 6 shows clearly the enhanced mixing effect due to the vortices generated near the conductive hurdles.

Improvement of designing the microfluidic mixers could benefit from numerical optimization methods for ICEO flows (Gregersen et al. 2009). Gregersen et al. (2009) numerically studied how the resulting ICEO flow depends on the topology and shape of the dielectric solid. They considered a dielectric solid surrounded by an electrolyte and positioned inside an externally biased parallel-plate capacitor. They extended conventional electrokinetic models with an artificial design field for the transition from the liquid electrolyte to the solid dielectric. With this design field, one can successfully apply the method of topology optimization to find system geometries with non-trivial topologies that maximize the net induced EOF rate through the electrolytic capacitor in the direction parallel to the capacitor plates.

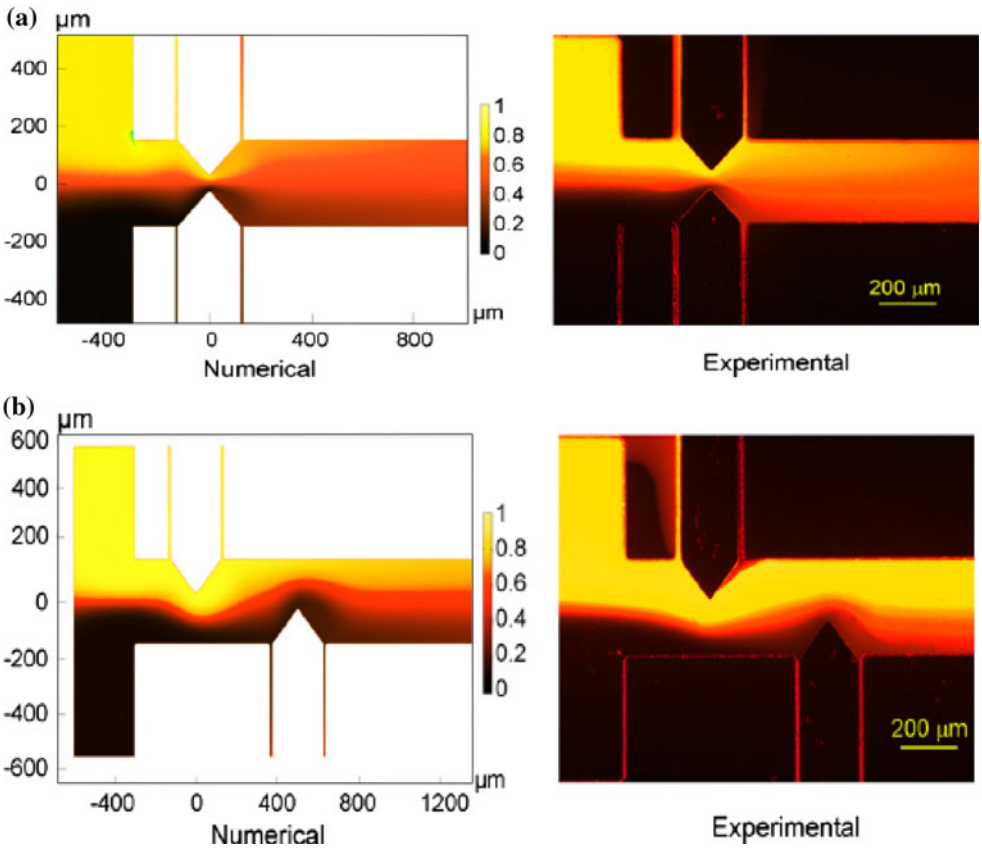

Fig. 6 Numerical simulation and experimental results of ICEOF enhanced mixing **a** with conductive platinum hurdles, **b** with non-conductive silicon hurdles (*source*: Wu and Li 2008b)

Recently, it was shown that the use of metallic microstructures (floating electrodes) to generate ICEO flows in microfluidic devices requires considerable care to avoid the unexpected electrokinetic coupling effects. A new phenomenon of ICEO flow was experimentally and theoretically demonstrated by Mansuripur et al. (2009). It was found that the capacitive coupling between a floating electrode and the external apparatus produces asymmetric flows in what would otherwise be symmetric systems. The potential drop between the applied potential, Φ_B, above the floating electrode and the (ground) potential of external conductors (e.g. the microscope stage) occurs across the double layer (with total capacitance $C_{DL}A_{DL}$) and across a stray coupling capacitor C_S (e.g. through the glass slide, where $C_s \sim \varepsilon_g A_e/d$). The stray double layer varies in phase with $\Phi_B(t)$, and thus with the parallel field $E_B(t)$, giving a non-zero time-averaged flow, much like fixed potential ICEO (Squires and Bazant 2004). Mansuripur demonstrated ways to manipulate or eliminate this flow through direct control of the 'external' potential or through geometric design of the mutual capacitance C_S.

3.2 ICEO pumps

Electro-osmosis (EO) is widely used as a pumping method in microfluidics (Laser and Santiago 2004) due to its significant advantages over the conventional pressure-driven flow, such as plug-like velocity profile, no moving parts and ease of being integrated within microchannels. However, there are several potential limitations, such as strong sensitivity to the surface and solution chemistry (which can cause flow reduction or reversal), and the need to sustain DC current through Faradaic reactions at the electrodes (resulting in typically unwanted effects, such as solution contamination, concentration gradients, electrode degradation, and bubble formation from hydrolysis). Because the electrostatic charge (zeta potential) of the non-conductive channel surfaces is low, DC-EOF requires applying high electric field, which resulting in some undesired effects (e.g. electrolysis and Joule heating). An alternative approach is to use the induced-charge EOF where the induced zeta potential can be controlled by the applied electric field and can be much higher than that in the case of electrostatic charge. In this area, AC electro-osmosis micropumps have been investigated extensively.

ACEO refers to the liquid motion generated initially at electrode surfaces when an AC field is applied. It typically happens at low frequency when the interfacial impedance dominates. Consider two planar electrodes that are placed parallel in an electrolyte solution. When an AC field is applied, the induced EDL on the positive electrode has negative net charge, and the EDL on the negative electrode

has positive net charge. In AC field, the double layer changes its polarity periodically. Since the tangential electric field changes its direction with the double-layer charges, steady flow and several vortices are produced above the electrodes. However, to transport liquid along a microchannel using AC-EOF, it is essential to break the symmetry of electric field around a pair of electrodes to produce a unidirectional flow. This can be achieved using either spatially asymmetric electrodes or polarization asymmetry. Figure 7a shows the concept of generating net flow using a pair of electrodes of unequal width, i.e., asymmetric electrodes. The surface flow velocity of asymmetric electrodes increases with decreased channel height, due to higher surface–volume ratio, and has a dependence on the square of the applied voltage, V^2 (Brown et al. 2001). Alternatively, breaking the symmetry can be achieved by inducing polarization asymmetry (Wu 2006). Figure 7b illustrates the principle of asymmetric polarization by applying a biased AC field to the two symmetric electrodes. The specially applied AC signal makes the left electrode always at a positive potential and the other electrode always at a negative potential. When the voltage exceeds the threshold for reaction, positive charges are induced on both the electrodes, and unidirectional flows are produced (Wu 2008).

It should be noted that the above-reviewed AC-EOF is not exactly the ICEK flow as we described previously in this article. This is because in AC-EOF the electrode itself is in contact with the liquid, it has a single uniform EDL, and there is no polarization process. In the ICEK systems, a conductor or a polarisable object is polarized by the applied electric field conducted via the liquid around it (not by the DC or AC power source directly). In this way, a multipolar induced EDL is formed around the conductor/polarisable object. If this polarization happens as a result of applying an AC field, then the induced-charge EOF is called the 'AC-ICEOF'. There are several ways to design AC-ICEOF pumps by breaking symmetry in a periodic electrode array. Experimental observations and theoretical models of AC-ICEOF were initially reported by many groups (Bikerman 1940; Dukhin and Derjaguin 1974; Rubinstein and Shtilman 1979; Bard and Faulkner 2001; Chu and Bazant 2005; Zaltzman and Rubinstein 2007; Suh and Kang 2008; Olesen 2006; Chu and Bazant 2007; Khair and Squires 2008; Gonzalez et al. 2008; Olesen et al. 2009). Ajdari (2000) suggested two ways to produce AC-ICEO flow, one is to modulate the electrode capacitance via a dielectric coating (Fig. 8a), another is to alternate the surface height (Fig. 8) with half the spatial period of the array, In these ways the one side of each electrode can generate a stronger AC-ICEO flow when compared to the other side and thus to produce a net pumping effect.

All the initial experimental works (e.g. Studer et al. 2004) and theoretical works (e.g. Olesen et al. 2006) on ICEOF pumping were focused on the design of Brown et al. (2001), co-planar electrodes with unequal widths and gaps. However, this design is inherently inefficient and prone to flow reversals due to the competition of opposing slip velocities. Bazant and Ben (2006) predicted theoretically that much faster and more robust flows can be generated by three-dimensional (3D) electrode shapes, which raise the forward slip velocities on steps and recess the reverse slip velocities in counter-rotating vortices, resulting in a 'fluid conveyor belt'. This idea can be implemented using a series of electrodes, each having a step change in height. On each electrode, the region to produce the desired forward flow is higher, while the region producing the reverse flow is lower, so as to re-circulate in a vortex aiding the forward flow (rather than fighting it, as in planar designs). This can be accomplished with electrodes having electroplated metal steps, as shown in Fig. 9, although other configurations are possible, such as flat electrode steps deposited on a grooved surface (without the vertical metal surfaces). Simulations predict that 3D AC-ICEOF pumps are faster than planar pumps by more than an order of magnitude (it can achieve mm/sec velocities with only a few volts), at the same voltage and with minimum feature size. Pumping by 3D AC-ICEOF arrays was investigated in experiments (Urbanski et al. 2006a, b) and simulations (Burch and Bazant 2008) Theoretically, the above-mentioned methods can enhance the electro-osmotic pumping significantly even by one order of magnitude; however,

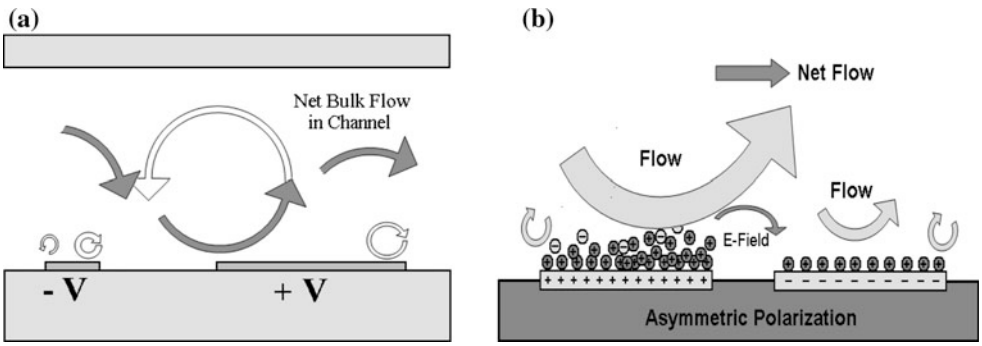

Fig. 7 Concept of generating net fluid transport by AC-EOF **a** by asymmetric electrodes **b** by asymmetric polarization

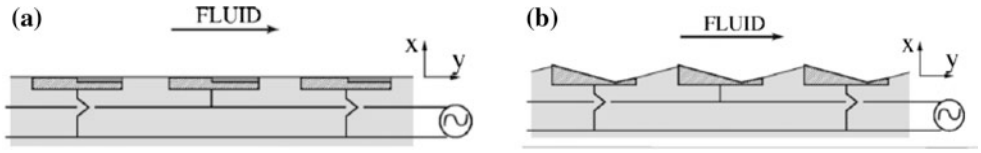

Fig. 8 Sketches of locally broken symmetries in a periodic electrode array which lead to global time-averaged ACEO pumping: **a** non-uniform surface coatings, **b** non-uniform surface height (*source*: Ajdari 2000)

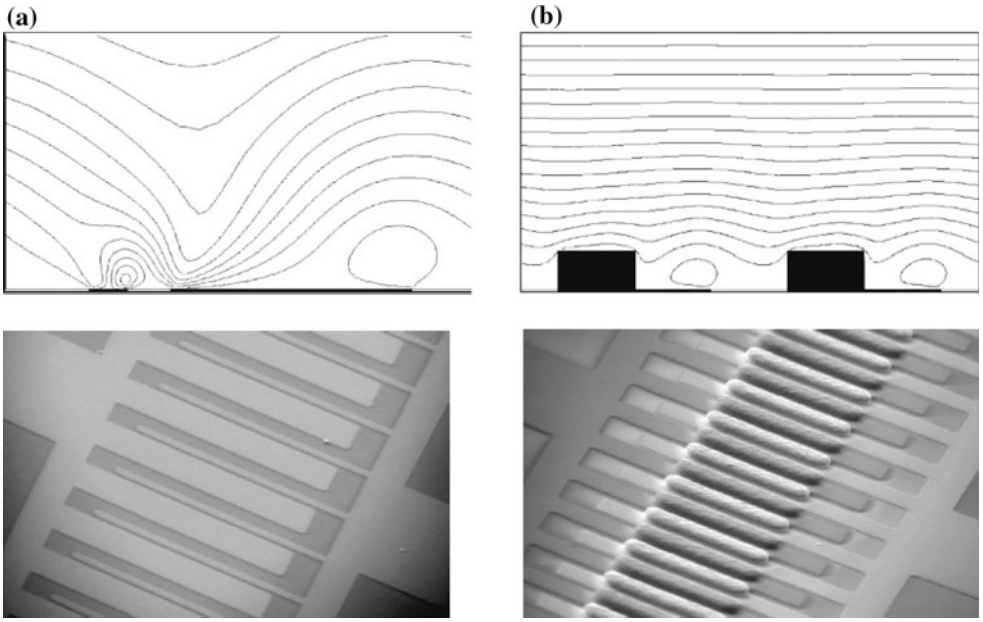

Fig. 9 *Top left* simulations of AC-ICEOF pump, showing the time-averaged flow over a pair of micro-electrodes (*dark regions*) in one spatial period of an interdigitated-electrode array. *Bottom left* array of planar electrodes with different sizes and gaps. *Top right* simulation of the AC-ICEO flow field over step-shaped electrodes, the 'fluid conveyor belt' (*source*: Bazant and Ben 2006). *Bottom right* SEM image of each design fabricated in gold on glass with minimum feature size (gap) of 5 μm (courtesy of Urbanski et al. 2006a, b)

manufacturing such systems is complicated, and the experimentally measured ICEOF velocities are on the order of several hundred microns per second only, similar to traditional DC-EOF.

4 ICEP

ICEP is the motion of a conductive or polarisable particle generated by the interaction of an applied electric field with the induced charge (and consequently the induced EDL) of the particle. The non-uniformly distribution of the induced EDL around the particle will cause non-uniform ICEO flow and vortices around the particle, which in turn lead to complex hydrodynamic interactions between the particle and the microchannel walls, and between particles. Asymmetry in particle shape and in polarizability can significantly alternate the induced-charge distribution and hence the induced EDL around the particle, consequently affecting the characteristics of the ICEP. In comparison with ICEOF, both theoretical and experimental studies of ICEP are limited.

4.1 Homogenous particle

As discussed before, when an electric field is applied to a conductive or polarisable particle, an induced dipolar EDL will be formed, as illustrated in Fig. 10a. The induced steady-state zeta potential on the particle surface ζ_p varies with position on the conductive surface. The EOF of the induced dipolar EDL will result in vortices near the particle surface. The interaction of the applied electric field and the static surface charge will create the electrophoretic motion of the particle. The vortices around the particle will affect the electrophoretic motion. In a microchannel, the situation will be even more complex. The electrostatic charges on the non-conducting channel walls will generate an EOF in the channel. The vortices around the particle will affect the flow field and interact with the channel walls. The net velocity of the particle will be determined by the electrophoretic motion of the particle, the bulk liquid EOF and the complex flow field (vortices) around the particle.

Bazant and Squires (2004) predicted that polarizable particles in the bulk can undergo essentially arbitrary translation and/or rotation by ICEP in a uniform electric field, as long as they possess appropriate broken

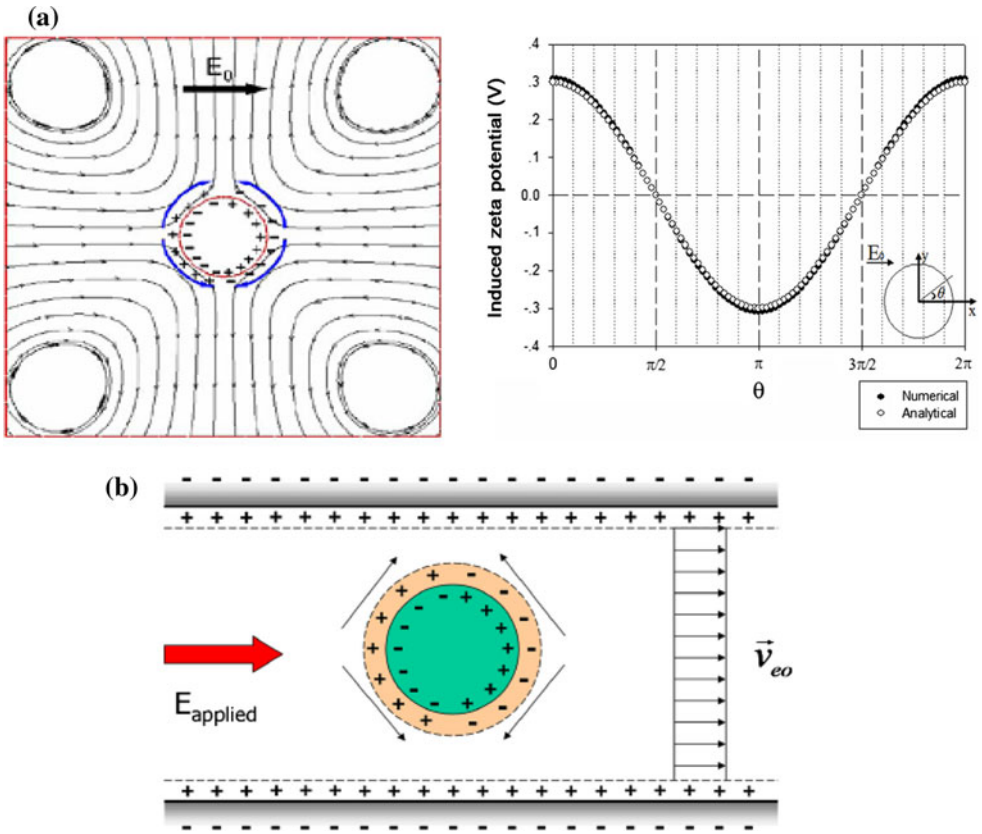

Fig. 10 **a** Induced-charge electroosmotic flow around an ideally polarizable particle, and the distribution of the induced zeta potential on a conductive circular cylinder surface, **b** ICEK motion of an ideally polarizable particle in a microchannel (*source*: Wu and Li 2009a)

symmetries (Squires and Bazant 2004) such as non-spherical shapes and/or non-uniform surface properties (e.g. due to coatings of different polarizability or compact-layer capacitance). ICEP can also contribute to the rotation of polarizable particles with elongated shapes (Bazant and Squires 2004; Yariv 2005; Saintillan et al. 2006a, b; Squires and Bazant 2006) as illustrated in Fig. 11. At low AC frequency (or in the DC limit), if the field persists in one direction long enough for ICEO flow to occur, then ICEP causes a rotational velocity which is independent of the particle size but sensitive to its shape (Squires and Bazant 2006).

ICEP is more sensitive to the particle shape and surface properties. If a polarisable particle has an asymmetric shape, the induced charges and the induced multi-polar EDLs will be non-symmetric. This can significantly influence the particle's motion, due to the alignment with the applied electric field and the unbalanced interactions of the induced vortices around the particle. Therefore, under the same applied electric field, polarisable particles of the same material and the similar sizes but different shapes will move in different directions at different speeds. However, these predictions require to be proved experimentally.

Many practical applications of electrophoresis require manipulating the motion of multiple particles. In such a situation, the electric field and the flow field surrounding

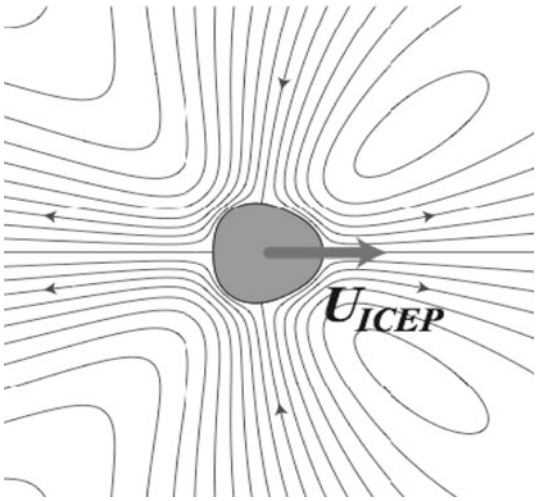

Fig. 11 An example of ICEO flow and resulting induced-charge electrophoretic velocity for an asymmetric shape (*source*: Squires and Bazant 2006)

one particle will be influenced by the presence of other particles nearby, and the induced-charge electrophoretic motion of polarizable particles will be transient generally. So far, there have been a few published works studying the ICEP particle–particle interactions with transient effects. However, the collective dynamics of colloids of polarizable particles in DC and low-frequency AC fields have been

studied. This was the motivation for the original analysis of 'ICEO' by Gamayunov et al. 1986, who predicted that the quadrupolar ICEO flow around two ideally polarizable spheres cause axial attraction along the field direction and radial repulsion from the equator. The transient alignment of asymmetric polarizable particles was also theoretically studied (Bazant and Squires 2004; Squires and Bazant 2004; Yariv 2005a, b; Squires and Bazant's 2006) and similar effect was found in the ICEP dynamics of rod-like metal particles (Rose et al. 2007). Such pair interactions have recently been observed for metallic rods in simulations by Saintillan et al. (2006a, b), who analysed far-field hydrodynamic interactions in the ICEP of colloidal rod dispersions using a statistical method, and in experiments by Rose et al. (2007). Furthermore, ICEP orientation of metallic rods was shown to suppress well-known sedimentation instability (Saintillan et al. 2006a, b; Hoffman and Shaqfeh 2009). Yossifon et al. (2007) studied the rotational ICEP motion of a polarizable dielectric spheroid in the presence of a uniform arbitrarily oriented external electric field. They illustrated symmetry breaking phenomena and demonstrate qualitative differences associated with variations of the dielectric constant. Regarding the ICEP rotation, they showed that a dielectric spheroid will approach an equilibrium orientation perpendicular to the electric field; while a freely suspended conductive spheroid will rotate to align its axis of symmetry with the external field.

Saintillan et al. (2006a, b) studied the behaviour of dispersions of ideally polarizable slender rods in an electric field, with and without Brownian motion. They proved that the effects of the non-linear induced-charge electrophoretic flows on the particle surfaces can be modelled by a linear slip velocity along the rod axes. This linear velocity causes the alignment of the rods in the direction of the electric field and induces linear distributions of point-force singularities. These distributions of point-forces disturb flow and result in hydrodynamic interactions. They also calculated the relative velocity between two aligned rods. The results showed that particle pairing can be expected as result of the relative motions. They had described a simulation method based on interactions between slender bodies, which include both far- and near-field hydrodynamic interactions as well as Brownian motion.

However, all the above-mentioned theoretical works developed the ICEP models using steady-flow approximations. There was no published work conductive complete 3D transient numerical simulation of ICEP motion of ideally polarizable particles until 2009. Recently, Wu and Li (2009; Wu et al. 2009) represented numerical studies of 3D transient movement of ideally polarizable spherical particle in an external electric field. They illustrated how two spherical polarizable particles interact with each other when the direction and strength of electric field changes. A complete three-dimensional time-dependant coupled multi-physics model is set up to describe the non-linear ICEP phenomena, which combines the basic principles of continuum liquid flow, induced-charge EDL, electro-osmosis and electrophoresis. The unique attracting and repelling effects between two polarizable conductive particles in an unbounded liquid and the corresponding effects of the particles' separation distance, the electric field strength and the particle size were discussed in their article (Wu and Li 2009). The numerical simulations indicate that an induced non-uniform zeta potential distribution on the conductive surface causes circulating flows near the particle. An attracting effect between the two polarizable conductive particles can be obtained when the electric field is applied parallel to the imaginary line connecting the two particles; while a repelling effect occurs when the applied electrical field is perpendicular to the imaginary line connecting the two particles (see Fig. 12). This is because of the non-symmetric vortexes generated between the two particles when they are positioned sufficiently close to each other. Under a parallel electric field, the microvortexes are inward rotating, inducing a low-pressure zone between the two particles, attracting the particles to get closer. Under a perpendicular electric field, the vortexes are outward rotating, inducing a high-pressure zone between the two particles, repelling the particles from each other.

When particles move through a relatively small microchannel, the existence of the channel wall will influence the particles' electrophoretic motion. Very little is known for the electrophoretic behaviour of electrically conductive and polarizable particles in such a small microchannel. For real microfluidic applications, the change of microchannel geometry (i.e. size and turns) and the particle's position to the wall will change the local electric field, and hence the ICEP motion of polarizable particles will be transient generally. Additionally, the existence of channel wall will produce EOF and definitely affect the particle motion. So far, there are a few published works studying the wall effects on ICEP. Levitan et al. (2005) studied the perturbation of the ICEO flow around a metal cylinder in contact with an insulating wall in a slit microchannel and Zhao and Bau (2007a, b) analysed a similar problem with a 2D ideally polarizable cylindrical particle positioned next to a planar surface under both the thin and the thick double-layer approximations and calculated the electrostatic and hydrodynamic forces on the particle. However, both the works did not consider the cylinder's motion. None of these previous works considered the 3-D transient motion of ideally polarizable particles and all of them developed the ICEP models using steady-flow approximations. Recently, Kilic and Bazant (2007) theoretically studied ICEP motion of polarizable particles with wall interactions.

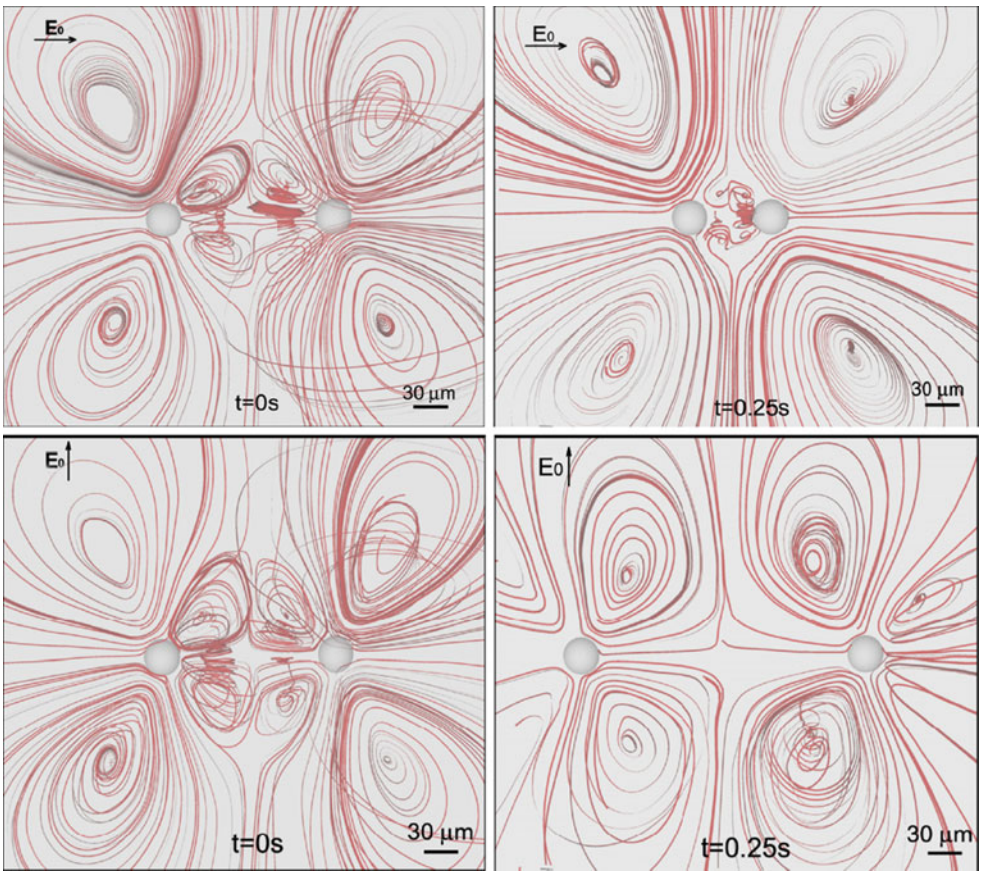

Fig. 12 ICEP motion of the two identical polarizable conductive spheres under parallel and perpendicular applied electric fields ($E_0 = 100$ V/cm, $d = 30$ μm) (*source*: Wu and Li 2009a)

However, the study was limited to quasi-steady analysis of particle's motions using STOKES flow and force-balancing approximations with no consideration of transient-coupled particle–fluid interactions. In 2009, Wu and Li represented a 3D modelling and numerical simulation of transient ICEP in a microchannel. In addition to the flow field, their model of the particle motion is based on the Newtonian force balances. The particle carries both the induced surface charge and the electrostatic charge; there is electric force acting on the particle by the applied electric field. At the same time, the flow field around the particle exerts a hydrodynamic force on the particle. The net force acting on the particle is given by Ye and Li (2004):

$$\vec{F}_{\text{net}} = \vec{F}_{\text{E}} + \vec{F}_{\text{h}} \tag{14}$$

where F_{E} is electrostatic force and F_{h} is the total hydrodynamic force, which combines two components

$$\vec{F}_{\text{h}} = \vec{F}_{\text{ho}} + \vec{F}_{\text{hin}} \tag{15}$$

where F_{ho} is the hydrodynamic force acting on the particle by the liquid flow in the region outside the EDL, and F_{hin} is the hydrodynamic force acting on the particle by the liquid flow in the region inside the EDL.

In their model, thin EDLs is considered, and the effect of flow field in the EDL is replaced by the electro-osmotic velocity as a slipping flow boundary condition for the flow field in the region outside the EDL. In this way, the flow field around the particles is the flow field originated outside the EDL and subject to the slipping flow boundary condition at the particle surface. Under this assumption, it can be shown that the F_{E} is balanced by F_{hin}, and the net force on the particle is thus given by (Ye and Li 2004):

$$\begin{aligned}\vec{F}_{\text{net}} = \vec{F}_{\text{ho}} &= \vec{G} - \oint_{\Gamma} \sigma_{\text{p}} \cdot \vec{n}\, \mathrm{d}S \\ &= (\rho - \rho_{\text{p}}) g V_{\text{p}} - \oint_{\Gamma} \sigma_p \cdot \vec{n}\, \mathrm{d}S\end{aligned} \tag{16}$$

and the total torque acting on the particle is given by

$$T_{\text{net}} = -\oint_{\Gamma} \left(\vec{x}_{\text{p}} - \vec{X}_{\text{p}}\right) \times (\sigma_p \cdot \vec{n})\, \mathrm{d}S \tag{17}$$

where $\vec{G}$ is the total body force, ρ_{p} is the density of the particle, V_{p} is the volume of the particle, g is acceleration due to gravity and σ_p is the stress tensor given by

$$\sigma_p = -p\vec{\vec{I}} + \mu\left[\nabla\vec{u} + (\nabla\vec{u})^T\right] \tag{18}$$

where $\vec{\vec{I}}$ is identity tensor.

The Newton's second law governs the particle motion, and is given by

$$m_{\mathrm{p}}\frac{\mathrm{d}\vec{V}_{\mathrm{p}}}{\mathrm{d}t} = \vec{F}_{\mathrm{net}} \tag{19}$$

$$J_{\mathrm{p}}\frac{\mathrm{d}\vec{\omega}_{\mathrm{p}}}{\mathrm{d}t} = \vec{T}_{\mathrm{net}} \tag{20}$$

where m_{p}, J_{p}, ω_{p} and T_{net} are the mass, momentum, rotational velocity and torque of the particle, respectively. The displacement of the particle centre is given by

$$\frac{\mathrm{d}\vec{X}_{\mathrm{p}}}{\mathrm{d}t} = \vec{V}_{\mathrm{p}} \tag{21}$$

The initial conditions of the particle motion and the flow velocity are set as zero.

To study the channel wall effects on the electrophoretic motion of the induced-charge particles, Wu and Li (2009) considered that a conductive spherical particle of 30 μm in diameter was placed at a distance of 15 μm from the bottom channel wall. To investigate the pure induced-charge effects, they did not consider any electrostatic charge on the particle surface. Their simulation showed significant lifting effect that brings the polarizable particle from the region near the wall to the centre of the channel, because of interaction of the vortices generated by the induced dipolar EDL around the particle with the channel walls. Figure 13 shows a comparison of the motions of the induced-charge electrophoresis with the standard electrophoresis of a particle initially placed close to the channel wall. Due to the unbalanced interaction of the vortices with the channel wall, there is net lifting force acting on the conductive particle. Strictly speaking, if the particle is placed extremely close to the channel wall, the electric field between the particle and the channel wall will be highly distorted and dielectrophoretic (DEP) force will provide additional lifting on the particle. However, the DEP force may be effective only during a very short initial period when the particle is very close to bottom wall. The induced vortices will immediately lift the particles from the wall; and thereafter the gap between the particle and the wall is sufficiently large (e.g. the size of the vortices) so that non-uniformity of the electric field around the particles is sufficiently small and the DEP effect is negligible. The lifting effect in the ICEP depends on the electric field and the particle size. Higher electric field and larger particle size give stronger wall-repelling effect. The polarizable particles tend to move to the channel's centreline if the particles have the similar density as that of the liquid, making particle auto focusing possible. Particle's density will also affect its final steady level of the ICEP motion in the microchannel. This provides a potentially effective way for particle separation by density.

4.2 Heterogeneous particle

Much less attention has been paid to the ICEK motion of heterogeneous particles, which have non-symmetrical shapes and/or non-uniform physical properties. The canonical example is that of a Janus particle with one metallic and one insulating hemisphere (Squires and Bazant 2006). In response to an applied electric field, the Janus particle rotates to align the interface between the two hemispheres with the electric field axis, due to both ICEP and DEP (dielectrophoresis). At the same time, for any orientation, the particle translates in the direction of its insulating end, propelled by ICEO flow on the metallic end, with a velocity

$$u = \frac{9\varepsilon R E^2}{64\,\mu(1+\delta)} \tag{22}$$

where R is the particle radius and δ is a dimensionless measure of the compact-layer capacitance. When the particle aligns in the field, it moves perpendicular to the electric field, with an azimuthal angle set by its initial orientation. This will be the case if the particle's insulating end is smaller or larger than the metallic end, since such a motion is determined by the broken symmetry. This may be understood by considering the ICEO flow in Fig. 14a. After alignment in the field, part of the usual quadrupolar ICEO flow is suppressed on the insulating end. The remaining ICEO flows over the metallic end sucks in fluid along the field axis and pushes it outward from the metallic pole, as shown in Fig. 14b, which propels the particle towards the insulating pole. Translation perpendicular to a

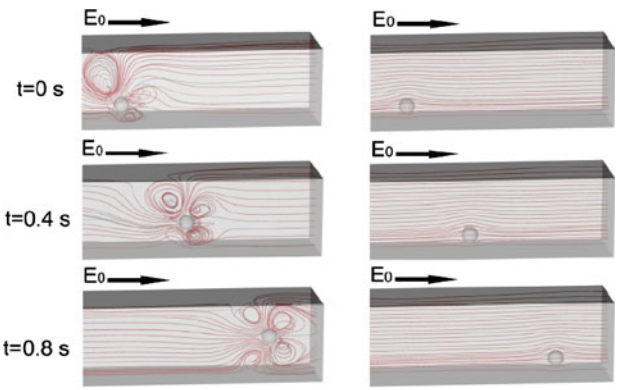

Fig. 13 Three-dimensional electrophoretic motion of **a** an ideally polarizable particle **b** a non-conductive particle in a microchannel (particle diameter $d = 30$ μm, channel width and height: $W = H = 150$ μm, $E_0 = 100$ V/cm) (*source*: Wu et al. 2008b)

DC field or continuous rotation for non-spherical shapes was first predicted by Long and Ajdari (1998). Perhaps the simplest example of ICEP is a spherical, metallo-dielectric Janus particle. In a free solution, the particle rotates to align the metal/dielectric plane with the applied field, while translating towards its dielectric end, ultimately translating perpendicular to the field (Squires and Bazant 2006).The Janus particle may form by cover one side of polarizable particle with non-conductive shield (Fig. 14a), or by combining a conductive material with another non-conductive material (see Fig. 14c). As shown in Fig. 14, the motion results from losing half of the ICEO quadrupolar flow on the dielectric side in comparison with a symmetric metal sphere, making the metallic side act as an 'engine'. However, none of the above-mentioned studies considered the electrostatic charge on the non-conductive section of Janus particle.

Since such a Janus particle tends to move towards its less polarizable end, a set of three Janus particles connected by rigid rods, as shown in the figure below, can generate continuous spin-wheel motion. This ICEP spin-wheel motion responds to DC and low-frequency AC electric fields. Perhaps such a set of particles could be used as a micromotor. Figure 15 illustrates an example which suggests how to design particles that spin continuously in a uniform field, as proposed by Squires and Bazant (2006).

Transverse ICEP motion of metallo-dielectric Janus particles in a uniform AC field has recently been observed by Gangwal et al. (2008). Consistent with theoretical predictions in Fig. 14, the particles align and translate perpendicularly to the field in the direction of the less polarizable (light) end. Their report is the first experimental observation of transverse electrophoresis of metallo-dielectric Janus particles (latex microspheres, half coated with gold). As shown in Fig. 16, the particles were observed to translate steadily in the direction perpendicular to a uniform AC field. In pure water and in dilute NaCl

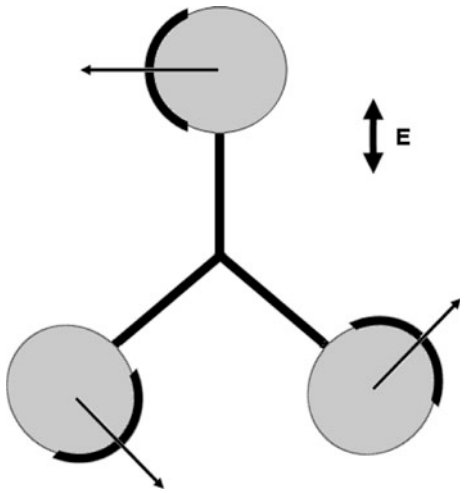

Fig. 15 An ICEP pinwheel, consisting of three Janus particles connected by rigid rods, which tilts to align and then spins continuous around the field axis

solutions, the motion follows the predicted scaling $u_{ICEP} \propto \varepsilon RE^2/\eta$. The larger particles move faster than the smaller ones. The ICEP velocity decays at higher ionic concentration, extrapolating to zero around 10 mM. The same concentration dependence is also observed in AC EOF. This motion is believed to be indeed due to ICEP. Significant departures from the theory were observed with increasing salt concentration ($c > 1$ mM) and/or with increasing voltage applied across the particles ($V > 0.1$ V). The motion became too slow to be observed at above 10-mM salt concentration.

A surprising aspect of these experiments was the strong interaction of the Janus particles and the glass walls of the microchannel (Kilic and Bazant 2007; Zhao and Bau 2007a, b). Although symmetric polarizable particles are expected to be repelled from insulating walls (Zhao and Bau 2007a, b; Wu and Li 2009), the Janus particles were attracted to the surface and observed moving parallel to the

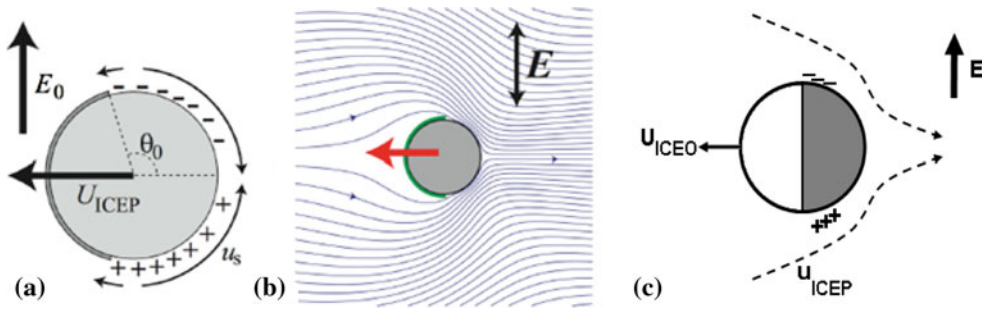

Fig. 14 Induced-charge electrophoresis of Janus particles, **a** stable orientation of a metal particle partially coated with an insulating thin film in a uniform field, showing induced charge and slip velocities on the metallic side, and the resulting motion toward the insulating end, perpendicular to the field. **b** Streamlines of two-dimensional ICEO flow around a Janus particle with a coated film on one half of its surface. **c** ICEP motion of a Janus particle formed by a conductive material with another non-conductive material (*source*: Squires and Bazant 2006)

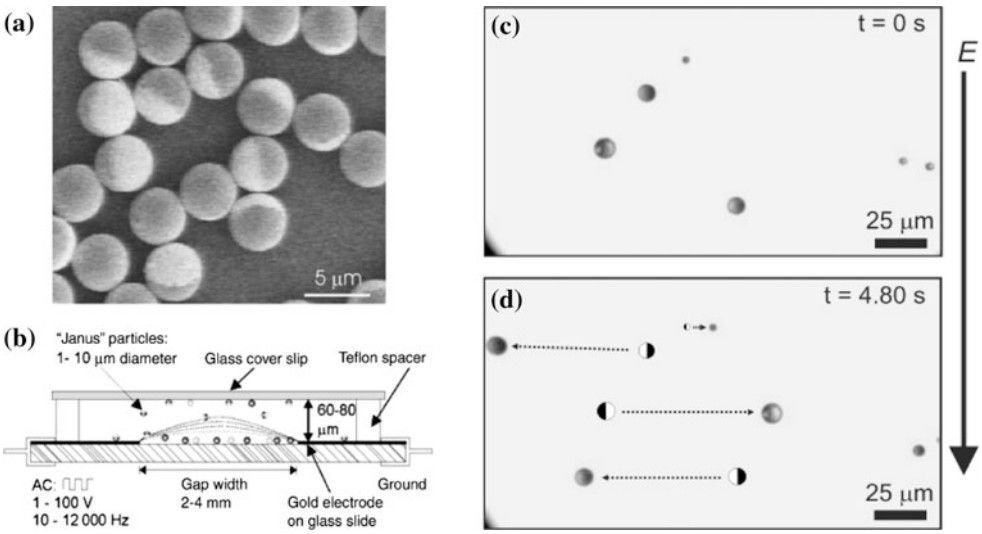

Fig. 16 Experimental observation of ICEP of metallo-dielectric Janus particles in a uniform 10 kHz AC field. **a** SEM image of 4.0-μm polystyrene particles partially coated with gold (the *brighter side*). **b** Schematic of the experimental set-up (not to scale). (**c**, **d**) Sequence of micrographs demonstrating motion transverse to the field in the direction of the dielectric (*light*) end propelled by the metallic (*dark*) end (*source*: Gangwal et al. 2008)

surface, very close to it (apparently within a particle diameter). The wall attraction has been attributed to hydrodynamic torque (Kilic and Bazant 2007) which rotates the dielectric end towards the wall, causing the Janus particle to swim towards it until a collision, and in some cases translate along the wall with a stable tilt angle around 45°. This example shows the rich possibilities of ICEP in confined geometries, which we believe merit further exploration. Anisotropic polarizable particles, such as Janus spheres, would exhibit more subtle many-body correlations and new possibilities for self assembly.

5 Second-kind EK

Generally, the ICEK phenomena are effective when the total (initial electrostatic and the induced) zeta potential is small. When this condition is violated, as in highly charged colloids, surface conduction leads to other 'non-equilibrium electro-surface phenomena' (NESP) (Dukhin 1993). Also, at very large voltages (above a limiting current) bulk space charge may also produce 'second-kind electrokinetic phenomena' (Mishchuk and Takhistov 1995) such unordinary effects may be useful in microfluidics (Ben and Chang 2002).

In the above, we considered the 'blocking' surfaces which the electric filed cannot pass through them. However, if considering a surface that allows the electric field enters into it, then the ICEO flow can be significantly modified. The electric conduction will 'short-circuit' the capacitive charging mechanism, so the time-dependent AC-ICEO flow tends to be reduced by Faradaic reactions. In the case of using steady DC voltage, the current into a surface can deplete the bulk salt concentration, causes concentration polarization and diffusion-osmosis (slip driven by bulk concentration gradients). Under the diffusion-limited current, if we apply large voltage to nearly deplete the bulk phase, then the diffuse-charge in the electrical double layer loses thermal equilibrium and expands into the bulk. Passing that limit causes the formation of extended space charge, which can alter the nature of ICEO flow. Under the condition of super-limiting current, the density of counter-ions in the electrical double layer loses its classical quasi-equilibrium profile. Therefore, a region of dilute space charge extends into the solution to the point where the bulk salt concentration becomes significant. Papers by Dukhin (1986) and Dukhin and Murtsovkin (1986) are the first studies of the nonlinear electro-osmotic flow driven by non-equilibrium space charge at large currents. He named this phenomena as 'electro-osmosis of the second kind' to distinguish it from electrokinetic phenomena of the first kind, whether linear or non-linear. If a particle is capable of keeping up with a super-limiting current, it will move by means of electrophoresis of the second kind. The second-kind electrophoresis has been observed experimentally for large (>10 μm) particles composed of cation-selective porous materials. Although the second-kind electrophoresis is much faster, a large applied electric field and strong surface/bulk chemical reactions are involved. These are major disadvantages of this phenomenon. As a result, the second-kind EK is not appropriate in most bio-medical applications.

6 Challenges and future research directions

ICEK phenomena are relatively new in microfluidics. ICEO can be used for pumping and mixing. ICEP leads to complicated new behaviour of polarizable particles in

microfluidic systems. A key feature of these phenomena is the non-linear dependence on the applied electric field, because the induced zeta potential is also dependent on the applied electric field. This enables to produce a stronger electrokinetic effect under the same applied electric field in comparison with the linear (or the traditional) EK.

Currently there are difficulties and unknowns associated with the studies of ICEK phenomena. These are obstacles prevent the application of ICEK in microfluidic LOC devices. However, they are also the opportunities for future research in this area (Squires 2009).

- *Flow visualization*. The characteristics of the theoretical and numerical prediction of the ICEOF include the vortices around the polarisable/conductive surfaces due to the induced dipolar EDL. However, the vortices are extremely difficult to observe experimentally. For example, when using fluorescent trace particles, these charged particles quickly adhere to the polarized surface within a few seconds, and hence alternated the induced EDL and consequently the induced-charge EO flow field. How to visualize the vortices around the polarisable surfaces is a major challenge in the studies of the flow field of ICEOF and interactions of polarisable particles with walls and with each other.
- *Polarizability*. Essentially all theoretical models of ICEK phenomena assume the solid is ideally/perfectly polarizable. In practice, however, the solids and their surfaces are not perfectly polarisable. The degree of polarizability will no doubt significantly affects the initial charging process (e.g., charging time) and the charge as well as the charge distribution at the steady-state. It will influence the induced EDL and the induced zeta potential. It is important to consider the polarizability effect in the models of ICEK.
- *Effects of polarisable materials and electrolytes*. Related to the polarizability, it is worthwhile to note that almost all ICEK experiments used gold or platinum surfaces in dilute KCl or NaCl solution. This is primarily for two reasons: (1) maintain an inert and ideally polarizable surface and (2) employ a simplest electrolyte that is binary, relatively small and symmetric. Exploring additional electrode materials (e.g. other metals, oxides, semiconductors, conductive carbon), other electrolytes (larger, asymmetric or multivalent ions or polyelectrolytes) and solvents (non-polar or ionic liquids) would provide better understanding of the ICEK phenomena and enable the development of better theoretical models, potentially elucidating the mechanisms behind the theory, and explaining the experiment discrepancies.
- *Low measured ICEK velocities*. While the qualitative and scaling features of experimentally measured ICEK phenomena generally agree with theory, measured ICEK flow velocities are almost always smaller than expected, some by one to three orders of magnitude. This suggests that some fundamental physical or chemical ingredients are missing from the current model of ICEK.
- *Suppression by salt*. Experimentally measured ICEK phenomena reduce in magnitude with increasing electrolyte concentration, and typically are immeasurably small for concentrations in excess of 10 mM. Furthermore, ICEK velocities often depend upon the specific salt in solution. These observations stand in striking contrast with the theory, which indicates no such a direct dependence. Without overcoming this suppression, it will be difficult for ICEO to find widespread and straightforward use in many practical LOC devices (e.g. direct pumping or mixing of buffer solutions).
- *Surface contamination*. So far, it has been assumed that the surface of the conductive or polarisable object is perfectly clean, so that the entire difference between the 'bulk' potential and the induced charge surface occurs across the diffuse layer of the EDL, for producing an induced zeta potential. The conductor surface may, however, be contaminated, e.g. covered with a dielectric layer; in such a case, part of voltage drop is across the double layer, and the rest drops across the dielectric layer.
- *Stern layers*. Another assumption made for ICEK analysing is that the entire potential drop occurs across the diffuse layer. However, part of the potential should drop across the 'Stern' layer (immobilized counterions). The Stern layer is often treated as a constant capacitor C_s in series with the double-layer capacitor, and thus behaves like a dielectric contaminant layer on the surface. Considering the Stern layer may provides better evaluation of the induced zeta potential.
- *Electrostatic charge*. Generally one assumes that the initial 'native' electrostatic charge on the conductive or polarisable surface remains constant, when an electric field is applied; and the total zeta potential is simply the local native zeta potential plus the induced zeta potential. However, the charging process may alternate the electrostatic charge distribution on the surface.

Compared to the vast literature on linear EK, the study of ICEK phenomena is still in its early stage. Applications of ICEK are still largely unexplored. For example, ICEP phenomena could be used to separate polarizable particles based on the shape, size and surface properties, which cannot be accomplished using conventional electrophoresis. As another example, understanding of the ICEK motion of heterogeneous particles may provide opportunities to discover new phenomena and develop new microfluidic

technologies, such as micromotors and microvehicles for carrying 'cargo' (e.g. molecules and cells).

Acknowledgement The authors wish to thank the financial support of the Natural Sciences and Engineering Research Council (NSERC) of Canada through a research grant to D. Li.

References

Ajdari A (2000) AC pumping of liquids. Phys Rev E 61:R45–R48
Anderson JL (1989) Colloid transport by interfacial forces. Ann Rev Fluid Mech 21:61–99
Bard AJ, Faulkner LR (2001) Electrochemical methods. Wiley, New York
Bazant MZ (2008) Nonlinear electrokinetic phenomena. In: Li D (ed) Encyclopedia of microfluidics and nanofluidics, part 14, vol 14. Springer, New York, pp 1461–1470
Bazant MZ, Ben Y (2006) Theoretical prediction of fast 3d AC electro-osmotic pumps. Lab Chip 6:1455–1461
Bazant MZ, Squires TM (2004) Induced-charge electrokinetic phenomena: theory and microfluidic applications. Phys Rev Lett 92:066101
Bazant MZ, Squires TM (2010) Induced-charge electrokinetic phenomena. Curr Opin Colloid Interface Sci (in press)
Bazant MZ, Kilic MS, Storey B, Ajdari A (2009) Towards an understanding of nonlinear electrokinetics at large voltages in concentrated solutions. Adv Colloid Interface Sci 152:48–88
Ben Y, Chang HC (2002) Nonlinear Smoluchowski slip velocity and micro-vortex generation. J Fluid Mech 461:229–238
Bikerman JJ (1940) Electrokinetic equations and surface conductance. A survey of the diffuse double layer theory of colloidal solutions. Trans Faraday Soc 36:154–160
Brown ABD, Smith CG, Rennie AR (2001) Pumping of water with AC electric fields applied to asymmetric pairs of microelectrodes. Phys Rev E 63:016305
Burch DN, Bazant MZ (2008) Design principle for improved three-dimensional AC electro-osmotic pumps. Phys Rev E 77:055303(R)
Chu KT, Bazant MZ (2005) Electrochemical thin films at and above the classical limiting current. SIAM J Appl Math 65:1485–1505
Chu KT, Bazant MZ (2007) Surface conservation laws at microscopically diffuse interfaces. J Colloid Interface Sci 315:319–329
Dukhin AS (1986) Pair interaction of disperse particles in electric-field. 3. Hydrodynamic interaction of ideally polarizable metal particles and dead biological cells. Colloid J USSR 48:376–381
Dukhin AS (1993) Biospecific mechanism of double layer formation and peculiarities of cell electrophoresis. Colloids Surf A 73:29–48
Dukhin SS, Derjaguin BV (1974) Surface and colloid science, Chapter 2, vol 7. Academic Press, New York
Dukhin AS, Murtsovkin VA (1986) Pair interaction of particles in electric field. 2. Influence of polarization of double layer of dielectric particles on their hydrodynamic interaction in stationary electric field. Colloid J USSR 48(2):203–209
Gamayunov NI, Murtsovkin VA, Dukhin AS (1986) Pair interaction of particles in electric field. Part 1: features of hydrodynamic interaction of polarized particles. Colloid J USSR 48(2):197–203
Gamayunov NI, Mantrov GI, Murtsovkin VA (1992) Investigation of the flows induced by an external electric field in the vicinity of conducting particles. J of Colloid 54(1):26–30
Gangwal S, Cayre OJ, Bazant MZ, Velev OD (2008) Induced-charge electrophoresis of metallo-dielectric particles. Phys Rev Lett 100(5) Art No. 058302
Gonzalez A, Ramos A, Green NG, Castellanos A, Morgan H (2000) Fluid flow induced by non-uniform AC electric fields in electrolytes on microelectrodes. II. A linear double-layer analysis. Phys Rev E 61:4019
Gonzalez A, Ramos A, Garcia-Sanchez P (2008) A castellanos effect of the difference in ion mobilities on traveling wave electro-osmosis. IEEE Int Conf Dielectric Liquids 1–4. doi:10.1109/ICDL.2008.4622452
Green NG, Ramos A, Gonzalez A, Morgan H, Castellanos A (2000) Fluid flow induced by non-uniform AC electric fields in electrolytes on microelectrodes. I. Experimental measurements. Phys Rev E 61:4011–4018
Green NG, Ramos A, Gonzalez A, Castellanos A, Morgan H (2002) Fluid flow induced by non-uniform AC electric fields in electrolytes on microelectrodes. III. Observation of streamlines and numerical simulation. Phys Rev E 66:026305
Gregersen MM, Okkels F, Bazant MZ, Bruus H (2009) Topology and shape optimization of induced-charge electro-osmotic micropumps. New J Phys 11:075016
Harnett CK, Templeton J, Dunphy-Guzman K, Senousy YM, Kanouff MP (2008) Model based design of a microfluidic mixer driven by induced charge electroosmosis. Lab Chip 8:565–572
Hoffman BD, Shaqfeh ESG (2009) The effect of Brownian motion on the stability of sedimenting suspensions of polarizable rods in an electric field. J Fluid Mech 624:361–388
Hunter RJ (1981) Zeta potential in colloid science: principles and applications. Academic Press, New York
Hunter RJ (2001) Foundations of colloid science. Oxford University Press, Oxford
Khair AS, Squires TM (2008) Fundamental aspects of concentration polarization arising from non-uniform electrokinetic transport. Phys Fluids 20:087102
Kilic MS, Bazant MZ (2007) Induced-charge electrophoresis near an insulating Wall. arXiv:0712.0453
Laser DJ, Santiago JG (2004) A review of micro-pumps. J Micromech Microeng 14:R35–R64
Levich VG (1962) Physicochemical hydrodynamics. Prentice-Hall, Englewood Cliffs
Levitan JA, Devasenathipathy S, Studer V, Ben Y, Thorsen T, Squires TM, Bazant MZ (2005) Experimental observation of induced-charge electro-osmosis around a metal wire in a microchannel. Colloids Surf A 267:122–132
Li D (2004) Electrokinetics in microfluidics. Academic Press, New York
Li D (2008) Encyclopedia of microfluidics and nanofluidics. Springer, New York
Long D, Ajdari A (1998) Symmetry properties of the electrophoretic motion of patterned colloidal particles. Phys Rev Lett 8:1529–1532
Lyklema J (1995) Fundamentals of interface and colloid science. Volume II: solid-liquid interfaces. Academic Press, San Diego
Mansuripur T, Pascall AJ, Squires TM (2009) Asymmetric flows over symmetric surfaces: capacitive coupling in induced charge electro-osmosis. New J Phys 11:075030
Mishchuk NA, Takhistov PV (1995) Electroosmosis of the second kind. Colloids Surf A 95:119–131
Murtsovkin VA (1996) Nonlinear flows near polarized disperse particles. Colloid J 58(3):341–349
Olesen LH (2006) AC electrokinetic micro-pumps, Ph.D. thesis, Danish Technical University. http://www2.mic.dtu.dk/research/MIFTS/publications/PhD/PhDthesisLHO.pdf
Olesen LH, Bruus H, Ajdari A (2006) AC electrokinetic micropumps: the effect of geometrical confinement, faradaic current injection and nonlinear surface capacitance. Phys Rev E 73, Art. no. 056313
Olesen LH, Bazant MZ, Bruus H (2009) Strongly nonlinear dynamics of electrolytes in large ac voltages. Phys Fluid Dyn ArXiv: 0908.3501v1

Pascall AJ, Squires TM (2010) Induced charge electroosmosis over controllably-contaminated electrodes. Phys Rev Lett 104(8) (Art. no. 088301)

Ramos A, Morgan H, Green NG, Castellanos A (1999) AC electric-field-induced fluid flow in microelectrodes. J Colloid Interface Sci 217:420–422

Rose KA, Meier JA, Dougherty GM, Santiago JG (2007) Rotational electrophoresis of striped metallic microrods. Phys Rev E 75: 011503

Rubinstein I, Shtilman L (1979) Voltage against current curves of cation exchange membranes. J Chem Soc Faraday Trans II 75: 231–246

Saintillan D (2008) Nonlinear interactions in electrophoresis of ideally polarizable particles. Phys Fluids 20:067104

Saintillan D, Darve E, Shaqfeh ESG (2006a) Hydrodynamic interactions in the induced-charge electrophoresis of colloidal rod dispersions. J Fluid Mech 563:223–259

Saintillan D, Shaqfeh ESG, Darve E (2006b) Stabilization of a suspension of sedimenting rods by induced-charge electrophoresis. Phys Fluids 18(12):121503

Saville DA (1977) Electrokinetics effect with small particles. Annu Rev Fluid Mech 9:321–337

Schoch RB, Han JY, Renaud P (2008) Transport phenomena in nanofluidics. Rev Mod Phys 80(3):839–883

Simonov IN, Dukhin SS (1973) Theory of electrophoresis of solid conducting particles in case of ideal polarization of a thin diffuse double-layer. Colloid J USSR 35(1):191–193

Soni G, Squires TM, Meinhart CD (2007) Nonlinear phenomena in induced-charge electroosmosis: a numerical and experimental investigation. In: Viovy JL, Tabeling P, Descroix S, Malaquin L (eds) Micro total analysis systems, vol 1, Chemical and Biological Microsystems Society, pp 291–293

Squires TM (2009) Induced-charge electrokinetics: fundamental challenges and opportunities. Lab Chip 9(17):2477–2483

Squires MT, Bazant MZ (2004) Induced-charge electro-osmosis. J Fluid Mech 509:217–252

Squires TM, Bazant MZ (2006) Breaking symmetries in induced-charge electro-osmosis and electrophoresis. J Fluid Mech 560: 65–101

Stone H, Stroock A, Ajdari A (2004) Engineering flows in small devices: microfluidics toward a lab-on-a-chip. Annu Rev Fluid Mech 36:381411

Studer A, Pepin A, Chen Y, Ajdari A (2004) An integrated AC electrokinetic pump in a microfluidic loop for fast tunable flow control. Analyst 129:944–949

Suh YK, Kang S (2008) Asymptotic analysis of ion transport in a nonlinear regime around polarized electrodes under AC. Phys Rev E 77:011502

Thamida S, Chang HC (2002) Nonlinear electrokinetic ejection and entrainment due to polarization at nearly insulated wedges. Phys Fluids 14:4315

Urbanski JP, Levitan JA, Bazant MZ, Thorsen T (2006a) Fast AC electro-osmotic pumps with non-planar electrodes. Appl Phys Lett 89:143508

Urbanski JP, Levitan JA, Burch DN, Thorsen T, Bazant MZ (2006b) The effect of step height on the performance of AC electro-osmotic microfluidic pumps. J Colloid Interface Sci 309:332–341

Wang SC, Chena HP, Lee CY, Yu CC, Chang SC (2006) AC electro-osmotic mixing induced by non-contact external electrodes. Biosens Bioelectron 22(4):563–567

Wu J (2006) Electrokinetic microfluidics for on-chip bio-particle processing. IEEE Trans Nanotechnol 5(2):84–89

Wu J (2008) Interactions of electrical fields with fluids: laboratory-on-a-chip applications. IET Nanobiotechnol 2(1):14–27

Wu Z, Li D (2008a) Micromixing using induced-charge electrokinetic flow. Electrochim Acta 53(19):5827–5835

Wu Z, Li D (2008b) Mixing and flow regulating by induced-charge electrokinetic flow in a microchannel with a pair of conducting triangle hurdles. Microfluid Nanofluid 5:65–76

Wu Z, Li D (2009) Induced-charge electrophoretic motion of ideally polarizable particles. Electrochim Acta 54:3960–3967

Wu Z, Gao Y, Li D (2009) Electrophoretic motion of ideally polarizable particles in a microchannel. Electrophoresis 30:773–781

Yariv E (2005a) Electro-osmotic flow near a surface charge discontinuity. Phys Fluids 17:051702

Yariv E (2005a) Induced-charge electrophoresis of non-spherical particles. Phys Fluids 17, Art. no. 051702

Yariv E (2008) Slender-body approximations for electrophoresis and electro-rotation of polarizable particles. J Fluid Mech 613:85–94

Yariv E (2009) Boundary-induced electrophoresis of uncharged conducting particles: remote-wall approximations. Proc R Soc A 465:709–723

Ye C, Li D (2004) 3-D transient electrophoretic motion of a spherical particle in a T-shaped rectangular microchannel. J Colloid Interface Sci 272:480–488

Yossifon G, Frankel I, Miloh T (2006) On electro-osmotic flows through microchannel junctions. Phys Fluids 18:117108

Yossifon G, Frankel I, Miloh T (2007) Symmetry breaking in induced-charge electro-osmosis over polarizable spheroids. Phys Fluids 19:068105

Zaltzman B, Rubinstein BI (2007) Electro-osmotic slip and electro-convective instability. J Fluid Mech 579:173–226

Zhao H, Bau H (2007a) A microfluidic chaotic stirrer utilizing induced-charge electro-osmosis. Phys Rev E 75:066217

Zhao H, Bau H (2007b) On the effect of induced electro-osmosis on a cylindrical particle next to a surface. Langmuir 23:4053–4063